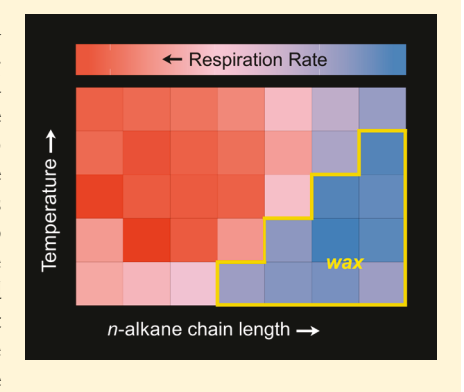


The Wax-Liquid Transition Modulates Hydrocarbon Respiration Rates in Alcanivorax borkumensis SK2

Li-Na Lyu, †,‡,§,|| Haibing Ding,†,⊥ Zhisong Cui,‡,§,# and David L. Valentine*,‡,§o

Supporting Information

ABSTRACT: Marine hydrocarbon biodegradation is an important environmental process conducted by microbes and modulated by oceanographic conditions. Following up on the patterns of petroleum hydrocarbon biodegradation observed after the Deepwater Horizon disaster, we measured respiration rates for the obligate alkane-degrading bacterium, Alcanivorax borkumensis SK2, to assess the relationship between hydrocarbon respiration rates and the phase, wax versus liquid, of the substrate. Using a matrix of temperatures (20, 25, 30, 35, and 40 °C) and n-alkanes $(n-C_{14}, n-C_{15}, n-C_{16}, n-C_{17}, n-C_{18}, n-C_{19}, and n-C_{20})$ for which each temperature gap spans the phase transition point of an n-alkane, we demonstrate that the n-alkane respiration rate decreases substantially when the substrate is in the wax versus liquid phase. The observed effect spans the full experimental temperature range. Subsequent experimentation with only wax-phase n-C₁₉ indicates that the availability of surface area modulates the n-alkane respiration rate and is likely a factor contributing to the



observed respiration rates being lower for wax-phase than for liquid-phase hydrocarbons. These results demonstrate that waxphase hydrocarbons are subject to biodegradation by A. borkumensis SK2 but that rates are suppressed relative to those of liquidphase hydrocarbons. The results are consistent with interpretations of hydrocarbon biodegradation patterns from Deepwater Horizon with broader relevance to the behavior of hydrocarbons in the ocean.

■ INTRODUCTION

Canonically, hydrocarbon biodegradation follows first-order kinetic behavior, with the magnitude of the rate constant being inversely proportional to the number of carbons and the structural complexity of the molecule being biodegraded. 1,2 Multicyclic molecules, such as hopane and sterane biomarkers and polycyclic aromatic hydrocarbons, are most resistant to biodegradation.³⁻⁶ In particular, the biomarker molecule $17\alpha,21\beta$ -hopane has been identified as a highly conserved compound to which other hydrocarbons are commonly referenced to enable calculation of biodegradation rates.⁷ However, following the Deepwater Horizon spill, steranes and hopanes were biodegraded more rapidly than expected. 9-11 In the case of hopane, biodegradation occurred at a rate similar to that of n- C_{32} and more rapid than those of n-alkanes > n- C_{32} , undermining the dogma that structural complexity controls hydrocarbon biodegradation kinetics in the marine offshore environment.11

On the basis of the observations from *Deepwater Horizon*, we asked if molecular weight might conditionally outweigh structural complexity in modulating biodegradation kinetics. We posited that one mechanism by which this might occur is through reduced bioavailability caused by the phase transition from liquid oil to solid wax. Formation of wax-phase hydrocarbon residues may have been facilitated in the case of Deepwater Horizon by the combination of a low ambient temperature (~5 °C) and preferential weathering (dissolution and biodegradation) of low-molecular weight components. 11-17

To test the effect of the wax- versus liquid-phase difference on hydrocarbon biodegradation, we chose Alcanivorax borkumensis SK2, a globally distributed marine hydrocarbon degrader. 18,19 Experimental design included replicated growth of A. borkumensis SK2 in a matrix of temperatures (20, 25, 30, 35, and 40 °C) and *n*-alkanes (*n*- C_{14} , *n*- C_{15} , *n*- C_{16} , *n*- C_{17} , *n*- C_{18} , n-C₁₉, and n-C₂₀), wherein each 5 °C temperature increment corresponded to the phase change of an n-alkane. By this design, we are able to disentangle the confounding effects of

Received: March 15, 2018 Revised: April 16, 2018 Accepted: April 17, 2018 Published: April 17, 2018

[†]College of Chemistry and Chemical Engineering, Ocean University of China, Qingdao, Shandong, China

[‡]Department of Earth Science, University of California at Santa Barbara, Santa Barbara, California 93106, United States

Marine Science Institute, University of California at Santa Barbara, Santa Barbara, California 93106, United States

State Key Laboratory of Organic Geochemistry, Guangzhou Institute of Geochemistry, Chinese Academy of Science, Guangzhou, China

 $^{^{\}perp}$ Key Laboratory of Marine Chemistry Theory and Technology, Ministry of Education, Ocean University of China, Qingdao, China *Marine Ecology Research Center, First Institute of Oceanography, State Oceanic Administration of China, Qingdao, China

temperature, substrate, and phase change on the respiration rate of *A. borkumensis* SK2.

■ MATERIALS AND METHODS

Strain, Chemicals, and Medium. The marine hydrocarbonoclastic bacterium, *A. borkumensis* SK2, used in our experiments was obtained from the German Collection of Microorganisms and Cell Cultures. All hydrocarbons used in our study were purchased from Acros Organics Co., and other chemicals were from Fisher Chemical Co. The purity for each of seven hydrocarbon substrates is 99%.

Culture medium ONR7a used in incubation experiments was prepared in a volume of 1 L, from three solutions. Solutions I and II were prepared and heat sterilized separately (121 °C, 25 min) and then mixed together after being cooled. Solution III was filter sterilized prior to mixing. Solution I contained 22.79 g of NaCl, 3.98 g of Na₂SO₄, 0.72 g of KCl, 83 mg of NaBr, 31 mg of NaHCO₃, 27 mg of H₃BO₃, 2.6 mg of NaF, 0.27 g of NH₄Cl, 89 mg of Na₂HPO₄·7H₂O, and 1.3 g of 3-{[1,3-dihydroxy-2-(hydroxymethyl)propan-2-yl]amino}-2-hydroxy-propane-1-sulfonic acid (TAPSO) and was adjusted to a pH of 7.6 by addition of a 12 M NaOH solution. Solution II contained 11.18 g of MgCl₂·6H₂O, 1.46 g of CaCl₂·2H₂O, and 24 mg of SrCl₂·6H₂O. Solution III contained 2.8 mg of FeSO₄·7H₂O.²⁰

Cultivation Conditions. To obtain inoculum for each experiment, *A. borkumensis* SK2 was grown on 25 μ L of liquid-phase n- C_{16} in 50 mL of ONR7a medium in the dark at 30 °C while being shaken at 150 rpm, to a final optical density of \sim 0.2 (Figure S1). Cells (4 mL) were harvested from the bottom of the growth vessel and homogenized by being gently shaken, and a 100 μ L inoculum of culture was added to 50 mL of fresh ONR7a medium for each experimental treatment. All incubation experiments were conducted using a New Brunswick Innova 44/44R Shaker.

Incubation Experiment Design. Two experiments were conducted in 250 mL sterile glass serum bottles sealed using a stopper with a PTFE-coated plug [Fisher Scientific, 7 mm (inside diameter) × 13 mm (outside diameter) at mouth] and an aluminum crimp and outfitted with an oxygen sensor spot (Pyroscience, OXSP5) to allow for remote monitoring of oxygen concentration (percent). The first experiment was designed with a matrix approach to evaluate the combined effects of the temperature, substrate, and physical phase of nalkanes on hydrocarbon respiration of A. borkumensis SK2. In this experiment, triplicate cultures of A. borkumensis SK2 were grown in 50 mL of ONR7a medium with 25 µL of a single nalkane substrate (0.05% by volume) added to each culture. The combination of seven *n*-alkanes (n- C_{14} , n- C_{15} , n- C_{16} , n- C_{17} , n- C_{18} , n- C_{19} , and n- C_{20}) and five different temperatures (20, 25, 30, 35, and 40 °C) forms the basis of the matrix (35 unique treatments, each in triplicate). Cultivation was conducted in the dark at 150 rpm for ~90 h. These n-alkanes were chosen for our experiment because their melting temperatures span the growth range for A. borkumensis SK2. The melting temperature of n-C₁₄, n-C₁₅, n-C₁₆, n-C₁₇, n-C₁₈, n-C₁₉, and n-C₂₀ are 5.9, 9.9, 18.2, 21, 28–30, 32–34, and 36.7 °C, respectively. ²¹ An alkane minus control was included at each temperature to exclude any effect from n-C₁₆ carryover from the A. borkumensis SK2

A second experiment was conducted to assess the effect of wax particle size on the growth of *A. borkumensis* SK2, using the apparatus as described above. For this experiment, two

treatments were included, with equal amounts of $n-C_{19}$ used as a carbon source in the form of wax. The first treatment contained the larger wax pieces that were formed by placing the uninoculated culture bottle with 50 mL of ONR7a medium into an ice bath for ~ 3 min and quickly adding 25 μ L of n-C₁₀. For the second treatment, uninoculated bottles with 50 mL of ONR7a medium and 25 μ L of n-C₁₉ were heated to 40 $^{\circ}$ C to convert the n-C₁₉ to liquid. Next the medium was sonicated for 30 min to form n- C_{19} microdroplets and then rapidly cooled in an ice bath to facilitate the formation of small wax particles. The visual appearance of wax in the two treatments at the onset of this experiment is shown in Figure S2. Both treatments were then inoculated with 100 µL of A. borkumensis SK2 and incubated at 25 °C on a rotary shaker in the dark at 150 rpm for 90 h. In this experiment, each treatment contained five replicates, with two of the replicates discarded from each treatment because they showed clear visible evidence of aggregation or disaggregation. For the two experiments described above, respiration rates were monitored by quantification of the oxygen concentration (percent) in the headspace at intervals of approximately 5-8 h.

Data Analysis and Calculations. For the first experiment, the oxygen consumption rates of A. borkumensis SK2 were obtained by linear regression using the three replicates for each treatment at each time point as well as using the mean values of three replicates. We fit the linear regression to the time interval representing the maximum sustained respiration rate, which followed a brief exponential phase of growth for the liquid substrate and spanned the entire duration of the incubation for the wax substrate. Calculations for liquid-phase alkanes with the exception of n-C₁₉ and n-C₂₀ utilized three to six measurements representing time windows of 24-54, 18-37, 18-34, 12-36, and 14-39 h at temperatures of 20, 25, 30, 35, and 40 °C, respectively. In contrast, 10-12 time points were used to calculate the maximum respiratory rates for wax-phase alkanes, corresponding to 24-92, 18-90, 18-92, 12-85, and 14-85 h for 20, 25, 30, 35, and 40 °C, respectively. For liquid-phase n-C₁₉ and n-C₂₀, linear regressions were also fit to the entire duration of the incubation. Doubling times were also estimated for the cultures, using the respiration time series as a proxy. Importantly, these calculations assume that per cell respiration rates are much higher for actively dividing cells than for cells in the stationary phase of growth. These calculations rely on oxygen time-series data bracketing the period of greatest exponential increase and assume standard bacterial growth behavior at this time. Growth curves of A. borkumensis SK2 on liquid alkanes are similar to traditional bacterial growth patterns (Figure S1).²⁰ Time points for calculating doubling times on liquid phases were selected from the early exponential phase, corresponding to 10-24, 13-18, 8-18, 0-18, and 0-19 h at 20, 25, 30, 35, and 40 °C, respectively. In contrast, plots of oxygen consumption versus time for wax-phase alkanes are approximately linear for the full duration. Therefore, these calculations used time ranges of 30-70, 25-70, 20-70, and 20-70 h at 20, 25, 30, and 35 °C, respectively. To calculate respiration rates for the second experiment, wherein variability was higher, we separately computed regression equations for each replicate and the ensemble.

■ RESULTS AND DISCUSSION

For the experiments described in this work, all combinations of temperature and *n*-alkane permitted sustained respiration by *A. borkumensis* SK2, whereas sustained respiration was insignif-

Environmental Science & Technology Letters

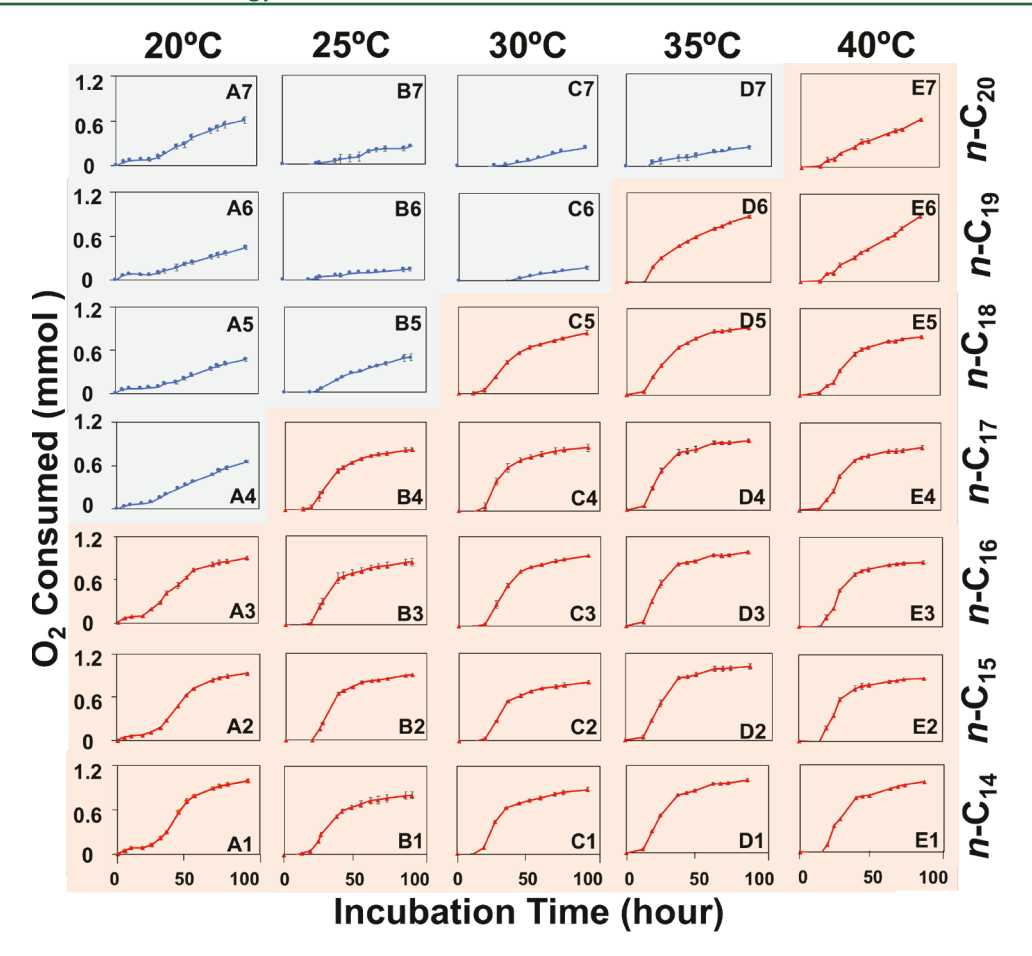


Figure 1. Time series of oxygen consumption for A. borkumensis SK2 growth in ONR7a medium, shown as a matrix of n-alkane versus temperature, as indicated. Columns are invariant for temperature, and rows are invariant for n-alkane substrate. The orange background corresponds to liquid alkanes; the gray background corresponds to wax-phase alkanes. All data are the mean of triplicate treatments, with error bars ($\pm 1\sigma$ standard deviation) provided.

icant in the control experiments. Figure 1 displays the time course of oxygen consumption in matrix form for all 35 incubation conditions, while Figure S14 displays the results from the alkane minus controls. The matrix approach to disentangle temperature, substrate, and phase change effects on the respiration rates of A. borkumensis SK2 reveals a clear effect associated with the alkane's phase and highlights the relatively more rapid respiration rates that accompany liquid-phase alkanes compared to those that accompany wax-phase alkanes. Notably, the respiration curves change in form across the waxliquid transition. For liquid alkanes, respiration curves display a clear exponential phase, followed by a sustained linear phase of maximal respiration, and then an asymptotic approach toward zero. In contrast, for wax-phase alkanes, the exponential phase has a shorter duration and subsequent respiration remains approximately linear for the duration of the incubation, suggesting that cell division was hindered by the unavailability of the substrate. This interpretation is supported by estimates of doubling time calculated by proxy from the respiration timeseries data (Figure 1). These calculations reveal doubling times on liquid-phase alkanes at optimum temperature similar to those previously reported, 22 whereas more protracted doubling times are calculated for growth on wax-phase alkanes (Table S1). Our interpretation of this observation is that A. borkumensis SK2 becomes substrate-limited when wax is present, which we attribute to surface area limitation likely

compounded by the difficulty of obtaining the alkane substrate from the solid phase.

The maximum respiration rates for each of the 35 treatments are displayed in the form of a heat plot, in Figure 2. Respiration rates on liquid-phase substrates ranged from 0.16 to 0.70 μ mol h^{-1} mL⁻¹, compared to a rate of 0.06–0.17 μ mol h^{-1} mL⁻¹ on the wax-phase substrate, spanning the full range of temperatures and substrates. This method of visualization highlights the impact of wax on respiration while also highlighting other metabolic features. The optimum range for temperature (25, 30, and 35 °C) and substrate (n- C_{14} , n- C_{15} , and n- C_{16}) is apparent by this approach and presumably reflects a combination of A. borkumensis' growth physiology and preferred catabolic pathways. Other subtle trends also emerge. Respiration rates appear to decline near the wax-liquid transition, including for conditions under which the substrate is in the liquid phase. The reason for this behavior remains uncertain but is perhaps related to physical structuring of the nalkanes near the wax transition point. Furthermore, A. borkumensis' complex regulatory network may trigger changes in metabolic preference, contributing to the observed patterns. Studies from the closely related Alcanivorax dieselolei reveal a regulatory network that varies with alkane chain length; the network involves sensing and uptake of alkanes, chemotaxis, and differential expression of genes encoding four different alkane hydroxylases. 23,24 Importantly, the four hydroxylase enzymes (P450, AlmA, and two AlkB homologues, AlkB1 and

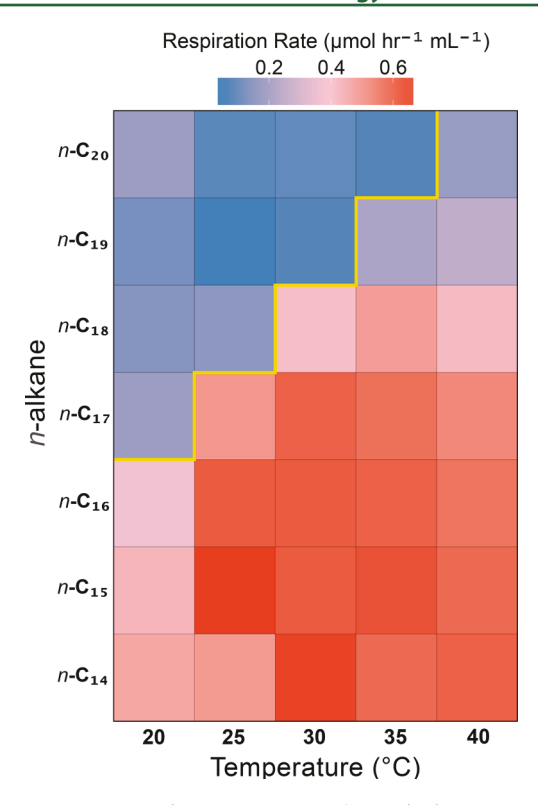


Figure 2. Heat map of respiration rates by *A. borkumensis* SK2 on seven alkanes at five temperatures. The yellow line denotes the phase boundary between the liquid and wax for the *n*-alkanes.

AlkB2) are also present in *A. borkumensis*¹⁹ and show chainlength dependence in their activity. By analogy with *A. dieselolei*, a shift in hydroxylase expression between P450 and the AlkB homologues is potentially relevant here, because *A. dieselolei* regulates expression of p450 according to $n\text{-C}_{14} = n\text{-C}_{16} > n\text{-C}_{18} > n\text{-C}_{20}$, for growth on pure alkane substrates.²³

Subtle differences in the calculated respiration rates are apparent in the data (Figures S3-S12) when applying different statistical approaches to the regressions. However, the results provided in Figure 1 and Figures S3-S12 are generally consistent with the interpretation that substrate availability modulates bacterial hydrocarbon consumption, with a significant discontinuity observed across the wax-liquid phase transition temperature and lower respiration rates for wax alkanes compared to liquid alkanes. While the hydrocarbons used in this study are insoluble in an aqueous solution, various adaptive mechanisms—the secretion of biosurfactants and direct cellular adhesion to hydrocarbon droplets-provide for cellular contact with extracellular hydrocarbons and are potentially important factors contributing to these results.^{25–29} In A. borkumensis SK2, perhaps the efficacy of such mechanisms is suppressed for the wax-phase substrate.

The results of our first experiment are consistent with respiration limited by cellular access to the wax-phase alkane substrate. To explore the importance of surface area contributing to respiration of *A. borkumensis* SK2, a second experiment was conducted wherein the wax-phase $n\text{-}C_{19}$ substrate was added as either a single particle or numerous small particles (see Figure S2). The results from this experiment demonstrate that the respiration rate of *A. borkumensis* SK2 is affected by the particle size distribution. Slower rates were found for the larger particle treatment (0.08 \pm 0.02 μ mol h⁻¹ mL⁻¹ versus 0.11 \pm 0.02 μ mol h⁻¹ mL⁻¹ per

Figure 3; 0.07 μ mol h⁻¹ mL⁻¹ versus 0.11 μ mol h⁻¹ mL⁻¹, p < 0.01, per Figure S13), and the distinction was found to be

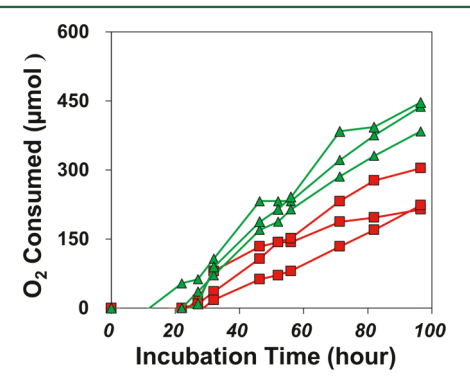


Figure 3. Time series of oxygen consumption for *A. borkumensis* SK2 grown on wax-phase n-C₁₉. Green lines display results for n-C₁₉ in the form of smaller particles, with a mean respiration rate of 0.11 \pm 0.02 μ mol h⁻¹ (mL of medium)⁻¹. Red lines display results for n-C₁₉ in the form of a single particle, with a mean respiration rate of 0.08 \pm 0.02 μ mol h⁻¹ (mL of medium)⁻¹. The error represents 1 σ SD.

statistically significant (p value of 0.005) using a two-sample t test. While the surface area of wax was not quantified in these experiments and indeed changed over the time course, the results are supportive of our assertion that surface area is a contributing factor modulating the respiration rate in the wax-phase substrate.

Our initial motivation for this work was to assess phase change effects on *n*-alkane respiration so as to inform observations of suppressed biodegradation for long chain *n*-alkanes (relative to isoprenoidal biomarkers) in the deep ocean following the *Deepwater Horizon* disaster. While our findings support a *Deepwater Horizon* biodegradation model that includes seafloor deposition of waxlike particles, ^{11,30} the processes by which such particles formed remain unclear. Several factors that likely contributed include dissolution of soluble hydrocarbons, biodegradation of labile hydrocarbons, a low ambient temperature, ballasting by adhesion to particles or bacterial flocculent, and surface aggregation effects of the resulting waxy particles.

In conclusion, A. borkumensis SK2 is able to grow on purely wax-phase n-alkanes, though it displays a substantially greater ability to grow on liquid-phase n-alkanes. The size of wax particles serves to modulate respiration, with slower rates for the larger particles. These observations are consistent with surface area being a contributing factor controlling the respiration rate for the wax substrate. These findings are also consistent with observations from the Deepwater Horizon disaster and suggest that wax formation might have contributed to the conditional recalcitrance of long chain *n*-alkanes in the deep ocean. Ramifications for the effect of wax precipitation on biodegradation extend beyond the Deepwater Horizon disaster to spills of wax-rich oils (e.g., Montara Spill), to the need for hydrocarbon compositional data to inform the decision process leading to application of chemical dispersant, and to biodegradation patterns for cyanobacterial hydrocarbons, pentadecane and heptadecane, in the open ocean.

■ ASSOCIATED CONTENT

Supporting Information

The Supporting Information is available free of charge on the ACS Publications website at DOI: 10.1021/acs.estlett.8b00143.

Growth pattern for A. borkumensis SK2 (Figure S1), visual appearance of wax-phase n-C₁₉ in culture media (Figure S2), linear regressions for the respiration rate of A. borkumensis SK2 on seven n-alkanes using the three replicates at each time point (Figures S3, S5, S7, S9, and S11), linear regressions for the respiration rate of A. borkumensis SK2 on seven alkanes using the mean value of the three triplicates at each time point (Figures S4, S6, S8, S10, and S12), linear regressions for the respiration rate of A. borkumensis SK2 on wax n-C₁₉ using the three replicates at each time point (Figure S13), time series of consumed oxygen for alkane minus controls (Figure S14), doubling time calculated by proxy from the respiration rate time series (Table S1), and all oxygen content (percent) data in the headspace of culture bottles for seven alkanes at five temperatures (Tables S2-S6) (PDF)

AUTHOR INFORMATION

Corresponding Author

*Department of Earth Science and Marine Science Institute, University of California, Santa Barbara, CA 93106. E-mail: valentine@ucsb.edu.

ORCID ©

David L. Valentine: 0000-0001-5914-9107

Notes

The authors declare no competing financial interest.

ACKNOWLEDGMENTS

Blair G. Paul provided assistance with data visualization. This research was supported by National Science Foundation Grants OCE-1333162 and OCE-1635562 (to D.L.V.); the National Natural Science Foundation for Creative Research Groups (Grant 41521064 to H.D.), China; the "111" Program Marine Chemistry (B13030); and Fundamental Funds for the Central Universities 201762030, China. L.-N.L. and Z.C. received support from the China Scholarship Council for their work at the University of California at Santa Barbara.

■ REFERENCES

- (1) National Research Council. Oil in the Sea III: Inputs, Fates, and Effects; National Academies Press: Washington, DC, 2003; p 446.
- (2) Wardlaw, G. D.; Nelson, R. K.; Reddy, C. M.; Valentine, D. L. Biodegradation preference for isomers of alkylated naphthalenes and benzothiophenes in marine sediment contaminated with crude oil. *Org. Geochem.* **2011**, 42 (6), 630–639.
- (3) Bossert, I. D.; Bartha, R. Structure-biodegradability relationships of polycyclic aromatic hydrocarbons in soil. *Bull. Environ. Contam. Toxicol.* **1986**, *37* (1), 490–495.
- (4) Butler, E. L.; Douglas, G. S.; Steinhauer, W. G.; Prince, R. C.; Aczel, T.; Hsu, C. S.; Bronson, M. T.; Clark, J. R.; Lindstrom, J. E. Hopane, a new chemical tool for measuring oil biodegradation. In *Onsite bioreclamation*; 1991.
- (5) Atlas, R. M.; Bartha, R. Hydrocarbon biodegradation and oil spill bioremediation. *Adv. Microb. Ecol.* **1992**, *12*, 287–338.
- (6) Bennett, B.; Larter, S. R. Biodegradation scales: applications and limitations. *Org. Geochem.* **2008**, *39* (8), 1222–1228.
- (7) Prince, R. C.; Elmendorf, D. L.; Lute, J. R.; Hsu, C. S.; Haith, C. E.; Senius, J. D.; Dechert, G. J.; Douglas, G. S.; Butler, E. L. $17\alpha(H)21\beta(H)$ -hopane as a conserved internal marker for estimating the biodegradation of crude oil. *Environ. Sci. Technol.* **1994**, 28 (1), 142–145.
- (8) Prince, R. C.; Douglas, G. S. Quantification of Hydrocarbon Biodegradation Using Internal Markers. In *Monitoring and Assessing*

- Soil Bioremediation; Springer: Berlin, 2005; pp 179–188, 10.1016/B978-0-12-803832-1.00019-2.
- (9) Aeppli, C.; Nelson, R. K.; Radovic, J. R.; Carmichael, C. A.; Valentine, D. L.; Reddy, C. M. Recalcitrance and degradation of petroleum biomarkers upon abiotic and biotic natural weathering of Deepwater Horizon oil. *Environ. Sci. Technol.* **2014**, *48* (12), 6726–6734.
- (10) Stout, S. A.; Payne, J. R.; Emsbo-Mattingly, S. D.; Baker, G. Weathering of field-collected floating and stranded Macondo oils during and shortly after the Deepwater Horizon oil spill. *Mar. Pollut. Bull.* **2016**, *105* (1), 7–22.
- (11) Bagby, S. C.; Reddy, C. M.; Aeppli, C.; Fisher, G. B.; Valentine, D. L. Persistence and biodegradation of oil at the ocean floor following Deepwater Horizon. *Proc. Natl. Acad. Sci. U. S. A.* **2017**, *114*, E9–E18.
- (12) Valentine, D. L.; Kessler, J. D.; Redmond, M. C.; Mendes, S. D.; Heintz, M. B.; Farwell, C.; Hu, L.; Kinnaman, F. S.; Yvon-Lewis, S.; Du, M.; Chan, E. W.; Tigreros, F. G.; Villanueva, C. J. Propane respiration jump-starts microbial response to a deep oil spill. *Science* **2010**, 330 (6001), 208–211.
- (13) Joye, S. B.; MacDonald, I. R.; Leifer, I.; Asper, V. Magnitude and oxidation potential of hydrocarbon gases released from the BP oil well blowout. *Nat. Geosci.* **2011**, *4* (3), 160.
- (14) Ryerson, T. B.; Aikin, K. C.; Angevine, W. M.; Atlas, E. L.; Blake, D. R.; Brock, C. A.; Fehsenfeld, F. C.; Gao, R.-S.; de Gouw, J. A.; Fahey, D. W.; Holloway, J. S.; Lack, D. A.; Lueb, R. A.; Meinardi, S.; Middlebrook, A. M.; Murphy, D. M.; Neuman, J. A.; Nowak, J. B.; Parrish, D. D.; Peischl, J.; Perring, A. E.; Pollack, I. B.; Ravishankara, A. R.; Roberts, J. M.; Schwarz, J. P.; Spackman, J. R.; Stark, H.; Warneke, C.; Watts, L. A. Atmospheric emissions from the Deepwater Horizon spill constrain air-water partitioning, hydrocarbon fate, and leak rate. *Geophys. Res. Lett.* **2011**, 38 (7), n/a.
- (15) Reddy, C. M.; Arey, J. S.; Seewald, J. S.; Sylva, S. P.; Lemkau, K. L.; Nelson, R. K.; Carmichael, C. A.; McIntyre, C. P.; Fenwick, J.; Ventura, G. T.; Van Mooy, A. S.; Camilli, R. Composition and fate of gas and oil released to the water column during the Deepwater Horizon oil spill. *Proc. Natl. Acad. Sci. U. S. A.* 2012, 109, 20229.
- (16) Ryerson, T. B.; Camilli, R.; Kessler, J. D.; Kujawinski, E. B.; Reddy, C. M.; Valentine, D. L.; Atlas, E.; Blake, D. R.; de Gouw, J.; Meinardi, S.; Parrish, D. D.; Peischl, J.; Seewald, J. S.; Warneke, C. Chemical data quantify Deepwater Horizon hydrocarbon flow rate and environmental distribution. *Proc. Natl. Acad. Sci. U. S. A.* **2012**, *109* (50), 20246–20253.
- (17) Valentine, D. L.; Mezić, I.; Maćešić, S.; Črnjarić-Žic, N.; Ivić, S.; Hogan, P. J.; Fonoberov, V. A.; Loire, S. Dynamic autoinoculation and the microbial ecology of a deep water hydrocarbon irruption. *Proc. Natl. Acad. Sci. U. S. A.* **2012**, *109* (50), 20286–20291.
- (18) Yakimov, M. M.; Golyshin, P. N.; Lang, S.; Moore, E. R.; Abraham, W. R.; Lünsdorf, H.; Timmis, K. N. *Alcanivorax borkumensis* gen. nov., sp. nov., a new, hydrocarbon-degrading and surfactant-producing marine bacterium. *Int. J. Syst. Bacteriol.* **1998**, 48 (2), 339–348.
- (19) Schneiker, S.; dos Santos, V. A. M.; Bartels, D.; Bekel, T.; Brecht, M.; Buhrmester, J.; Chernikova, T. N.; Denaro, R.; Ferrer, M.; Gertler, C.; Goesmann, A.; Golyshina, O. V.; Kaminski, F.; Khachane, A. N.; Lang, S.; Linke, B.; McHardy, A. C.; Meyer, F.; Nechitaylo, T.; Pühler, A.; et al. Genome sequence of the ubiquitous hydrocarbon-degrading marine bacterium *Alcanivorax borkumensis*. *Nat. Biotechnol.* **2006**, 24 (8), 997–1004.
- (20) Dyksterhouse, S. E.; Gray, J. P.; Herwig, R. P.; Lara, J. C.; Staley, J. T. *Cycloclasticus pugetii* gen nov., sp. nov., an aromatic hydrocarbon-degrading bacterium from marine sediments. *Int. J. Syst. Bacteriol.* **1995**, 45 (1), 116–123.
- (21) Dirand, M.; Bouroukba, M.; Briard, A.-J.; Chevallier, V.; Petitjean, D.; Corriou, J. P. Temperatures and enthalpies of (solid+solid) and (solid+liquid) transitions of n-alkanes. *J. Chem. Thermodyn.* **2002**, 34 (8), 1255–1277.
- (22) Naether, D. J.; Slawtschew, S.; Stasik, S.; Engel, M.; Olzog, M.; Wick, L. Y.; Timmis, K. N.; Heipieper, H. J. Adaptation of the hydrocarbonoclastic bacterium *Alcanivorax borkumensis* SK2 to alkanes

- and toxic organic compounds: a physiological and transcriptomic approach. Appl. Environ. Microbiol. 2013, 79 (14), 4282–4293.
- (23) Liu, C.; Wang, W.; Wu, Y.; Zhou, Z.; Lai, Q.; Shao, Z. Multiple alkane hydroxylase systems in a marine alkane degrader, *Alcanivorax dieselolei B-5. Environ. Microbiol.* **2011**, *13*, 1168–1178.
- (24) Wang, W.; Shao, Z. The long-chain alkane metabolism network of *Alcanivorax dieselolei*. *Nat. Commun.* **2014**, *5*, 5755.
- (25) Beal, R.; Betts, W. B. Role of rhamnolipid biosurfactants in the uptake and mineralization of hexadecane in *Pseudomonas aeruginosa*. *J. Appl. Microbiol.* **2000**, *89* (1), 158–168.
- (26) Ron, E. Z.; Rosenberg, E. Biosurfactants and oil bioremediation. Curr. Opin. Biotechnol. 2002, 13 (3), 249–252.
- (27) Golyshin, P. N.; Martins Dos Santos, V. A. P.; Kaiser, O.; Ferrer, M.; Sabirova, Y. S.; Lünsdorf, H.; Chernikova, T. N.; Golyshina, O. V.; Yakimov, M. M.; Pühler, A.; Timmis, K. N. Genome sequence completed of *Alcanivorax borkumensis*, a hydrocarbon-degrading bacterium that plays a global role in oil removal from marine systems. *J. Biotechnol.* **2003**, *106* (2–3), 215–220.
- (28) Sabirova, J. S.; Ferrer, M.; Regenhardt, D.; Timmis, K. N.; Golyshin, P. N. Proteomic insights into metabolic adaptations in *Alcanivorax borkumensis* induced by alkane utilization. *J. Bacteriol.* **2006**, *188* (11), 3763–3773.
- (29) de Carvalho, C. C.; Wick, L. Y.; Heipieper, H. J. Cell wall adaptations of planktonic and biofilm *Rhodococcus erythropolis* cells to growth on C5 to C16 n-alkane hydrocarbons. *Appl. Microbiol. Biotechnol.* **2009**, 82 (2), 311–320.
- (30) Valentine, D. L.; Fisher, G. B.; Bagby, S. C.; Nelson, R. K.; Reddy, C. M.; Sylva, S. P.; Woo, M. A. Fallout plume of submerged oil from Deepwater Horizon. *Proc. Natl. Acad. Sci. U. S. A.* **2014**, *111* (45), 15906–15911.